THE INFLUENCE OF COPPER ON THE DECARBURIZATION AND RECRYSTALLIZATION OF Fe-Si-Al ALLOYS

VPLIV BAKRA NA RAZOGLJIČENJE IN REKRISTALIZACIJO ZLITIN Fe-Si-Al

Darja Steiner Petrovič[1], Monika Jenko[1], Valter Doleček[2]

[1]Institute of Metals and Technology, Lepi pot 11, 1000 Ljubljana, Slovenia
[2]University of Maribor, Faculty of Chemistry and Chemical Engineering, Smetanova 17, 2000 Maribor, Slovenia

The decarburization and recrystallization of Fe-Si-Al alloys containing copper was investigated. The decarburization annealing of non-oriented electrical steel sheets produced from Fe-Si-Al alloys depends on the chemical reactions between the gas mixture and the carbon at the steel's surface. The carbon diffusion, the temperature of the decarburization annealing, the composition of the gas mixture and the chemical composition of the steel are the influencing parameters that determine the kinetics and the mechanism of decarburization. The decarburization of Fe-Si-Al alloys with the mass fraction of 0.24 % and 0.43 % of copper was compared with the decarburization of an Fe-Si-Al alloy with a very small amount of copper (0.01 %). The decarburization annealing was performed in a H_2-H_2O gas mixture at 840 °C. The residual carbon content was determined by analytical chemical method. The alloys were also recrystallized in hydrogen at 980 °C. Microstructure of the samples after decarburization and recrystallization annealing was investigated with optical microscopy.

Key words: decarburization, recrystallization, non-oriented electrical steels, copper, carbon

Preučevali smo razogljičenje in rekristalizacijo modelnih zlitin Fe-Si-Al z različno vsebnostjo bakra. Razogljičenje neorientiranih elektropločevin, ki jih lahko izdelujemo iz zlitin Fe-Si-Al, je odvisno od kemijskih reakcij med ogljikom, ki difundira na površino jekla, ter plinsko mešanico. Vplivni parametri, ki določajo kinetiko in mehanizem razogljičenja, so: površinska segregacija ogljika, temperatura razogljičevalnega žarjenja, sestava plinske mešanice in kemijska sestava jekla.

Razogljičenje smo merili v zlitinah Fe-Si-Al z vsebnostjo masnega deleža bakra 0,24 % in 0,43 % ter ga primerjali s tistim v zlitini z zelo nizko vsebnostjo bakra, 0,01 %. Zlitine smo razogljičili pri temperaturi 840 °C v plinski mešanici H_2-H_2O. Preostali delež ogljika po razogljičenju smo določili s kemijsko analizo vzorcev. Zlitine smo tudi rekristalizacijsko žarili v suhem vodiku pri 980 °C. Mikrostrukturo vzorcev po žarjenju za razogljičenje in rekristalizacijo smo analizirali s svetlobno mikroskopijo.
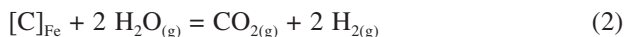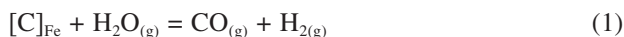
Ključne besede: rekristalizacija, razogljičenje, neorientirane elektropločevine, baker, ogljik

1 INTRODUCTION

Non-oriented electrical steel sheets, which are mainly used as the core material for motors and small transformers, are produced from silicon steel. Up to 1 % of Al can be added to the silicon steel to increase the electrical resistivity which decreases the eddy-current losses of the non-oriented steel. In the production of silicon steel, steel scrap is used. As a result, impurity elements such as Cu, Sn, Sb, Se, As and others can be found in the steel. Elements such as copper and tin can not be removed from the steel melt using current oxidation-refining processes.

The decarburization of silicon steel is one of the most important steps in the production of non-oriented electrical steel sheets and to achieve the optimum magnetic properties the carbon content of the steel sheets has to be lowered to at least 0.002 %. The decarburization is usually performed by annealing in a gas mixture of hydrogen and water vapour in the temperature range from 700 °C to 900 °C with a controlled partial pressure ratio of water vapour and hydrogen $p(H_2O)/p(H_2)$.

The chemical reactions of the decarburization of the steel in hydrogen containing water vapour are:

$$[C]_{Fe} + H_2O_{(g)} = CO_{(g)} + H_{2(g)} \tag{1}$$

$$[C]_{Fe} + 2\,H_2O_{(g)} = CO_{2(g)} + 2\,H_{2(g)} \tag{2}$$

$$[C]_{Fe} + 2\,H_{2(g)} = CH_{4(g)} \tag{3}$$

$$[C]_{Fe} + CO_{2(g)} = 2\,CO_{(g)} \tag{4}$$

The principal reaction that controls the decarburization is equation (1); the reaction according to equation (3) can be neglected when the $p(H_2O)/p(H_2)$ ratios are greater than 0.01.[1]

2 EXPERIMENTAL

The chemical composition of the laboratory-melted alloys is given in **Table 1**. The ingots were hot and cold rolled to sheets of thickness of 0.5 mm. From the steel sheets the specimens of $(80 \times 20 \times 0.5)$ mm were cut out and used for decarburization annealing. Specimens were introduced into the hot zone of the furnace, heated to the proper temperature in nitrogen, then the wet hydrogen-

gas mixture was introduced for the decarburization to occur.

w/%	C	Si	Al	Mn	Cu	P	S
VZ0_0,01	0.042	1.73	0.8	0.2	0.01	0.002	0.002
VZ1_0,24	0.011	1.90	0.5	0.2	0.24	0.005	0.005
VZ8_0,43	0.009	1.86	0.5	0.2	0.43	0.005	0.005

To saturate hydrogen with water vapour a water bath saturator was used. The temperature of the decarburization was $T = 840$ °C which is equal to that used in the industrial practice. The $p(H_2O)/p(H_2)$ ratio of the gas mixture was 0.05. After decarburization treatment for $t = 15$ min the samples were cooled down in dry hydrogen to room temperature. The recrystallization annealing was performed afterwards at $T = 980$ °C in dry hydrogen.

3 RESULTS AND DISCUSSION

The residual carbon content after decarburization is given in **Table 2**. It is obvious that the decarburization level was the highest in the sample with 0.01 % Cu, where the carbon content was lowered by more than 90 % of the initial value. However, considering the analytical method limitations, it is concluded, that the residual carbon contents in the decarburized steel was virtually the same for all three samples with different copper content. These residual carbon content is related to the equilibrium between the activity of carbon in the decarburizing atmosphere and in the steel at a given annealing temperature.

w(C) / %	VZ0_0,01	VZ1_0,24	VZ8_0,43
Initial carbon content	0.0420	0.0110	0.0090
Residual carbon content	0.0028	0.0025	0.0027

The reaction that controls the decarburization of silicon steel in the gas mixture H_2/H_2O at 840 °C is the oxidation of carbon, in which the carbon from the solid solution in the ferrite reacts with the water vapour. Reaction (1) is therefore the basic reaction that determines the decarburization kinetics. On the other
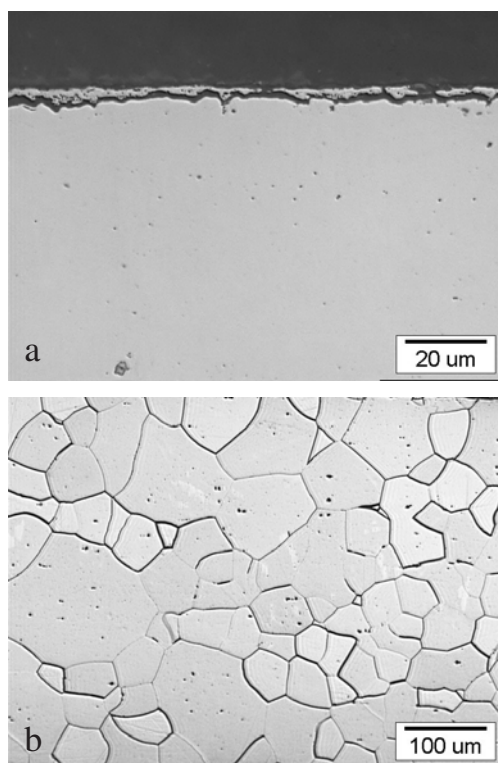
Figure 1: Microstructure of the Fe-Si-Al alloy with the mass fraction of Cu 0.24 % after decarburization annealing and recrystallization; a) oxide layer on the steel surface (mag. 500-times; non-etched), b) polygonal grains of ferrite in the microstructure of the steel (mag. 100-times; etchant: Nital)
Slika 1: Mikrostruktura zlitine Fe-Si-Al z masnim deležem bakra 0,24 % po žarjenju za razogljičenje in rekristalizacijo; a) oksidirana površina jekla (pov. 500-kratna; nejedkano), b) mikrostruktura jekla iz poligonalnih zrn ferita (pov. 100-kratna; jedkalo: nital)
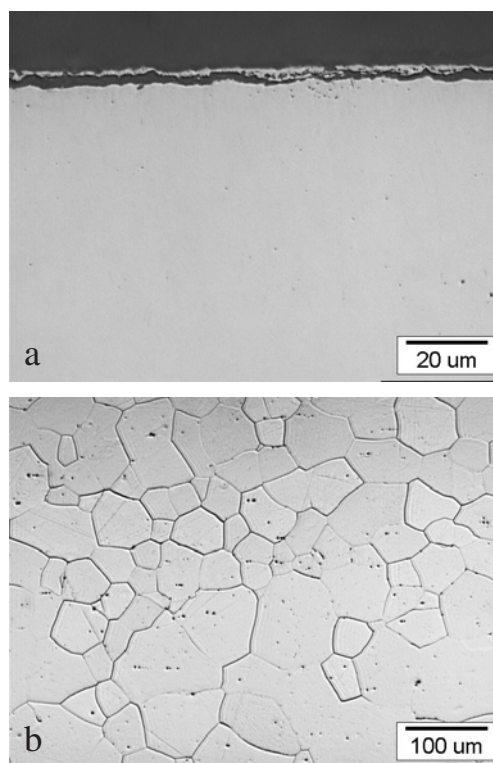
Figure 2: Microstructure of the Fe-Si-Al alloy with the mass fraction of Cu 0.43 % after decarburization annealing and recrystallization; a) oxide layer on the steel surface (mag. 500-times; non-etched), b) polygonal grains of ferrite in the microstructure of the steel (mag. 100-times; etchant: Nital)
Slika 2: Mikrostruktura zlitine Fe-Si-Al z masnim deležem bakra 0,43 % po žarjenju za razogljičenje in rekristalizacijo; a) oksidirana površina jekla (pov. 500-kratna; nejedkano), b) mikrostruktura jekla iz poligonalnih zrn ferita (pov. 100-kratna; jedkalo: nital)

hand, the partial pressure of oxygen in the gas mixture used for the decarburization was also sufficient for the oxidation of iron and the alloying elements on the specimen's surface that have a higher affinity towards oxygen than iron (Al, Si). For this reason, the surface of the silicon steel can be easily oxidized, even at very low dew points of the atmosphere [1,2,3].

In **Figures 1a,b-3a,b** the near surface regions and the microstructures of the specimens after the decarburization and recrystallization annealing are shown. **Figures 1a, 2a** and **3a** show the oxide layers on the surface and the layers of internal oxidation of the specimens. The oxide layer consists of Si, Al and Fe oxides as reported in the literature [1,2,3] and as confirmed in our previous works [4,5,6]. The oxidation of carbon and the alloying elements in the gas mixture H_2-H_2O at 840 °C are a function of the temperature and the oxygen potential of the atmosphere. The thickness of the oxide layer increases with the increasing time of the decarburization annealing. [4,5,6]

A difference was observed in the micromorphology of the subsurface regions of the alloys with different copper content. In the steel containing 0.01 % Cu small

Figure 3: Microstructure of the Fe-Si-Al alloy with a very low amount of copper (0.01 % Cu) after decarburization annealing and recrystallization; a) oxide and internal layers (mag. 500-times; non-etched), b) polygonal grains of ferrite in the microstructure of the steel (mag. 100-times; etchant: Nital)
Slika 3: Mikrostruktura primerjalne zlitine Fe-Si-Al z zelo nizko vsebnostjo bakra (0,01 % Cu) po žarjenju za razogljičenje in rekristalizacijo; a) oksidirana površina jekla in notranja oksidacija po kristalnih mejah (pov. 500-kratna; nejedkano), b) mikrostruktura jekla iz poligonalnih zrn ferita (pov. 100-kratna; jedkalo: nital)

inclusions produced by the internal oxidation were numerous (**Figure 3a**). The internal oxidation results from the reaction of oxygen dissolved in the steel matrix with elements with a higher free energy of the oxide formation than that of iron. Intergranular oxidation is a special case of internal oxidation in which the oxide inclusions form along the grain boundaries [7]. It is more frequent because the diffusivity of non-metal atoms is much faster than the volume diffusion.

The results for the Fe-3 % Si alloy [8] showed that in the region of $p(H_2O)/p(H_2) < 0.02$, oxygen stays on the alloy surface as an adsorbate but does not dissolve in iron, while at $p(H_2O)/p(H_2) > 0.025$, oxygen dissociated from water molecules in the gas phase was not only adsorbed on iron surface but was also dissolved in the iron base metal. This explains internal oxidation of the alloy at $p(H_2O)/p(H_2) > 0.025$.[8]
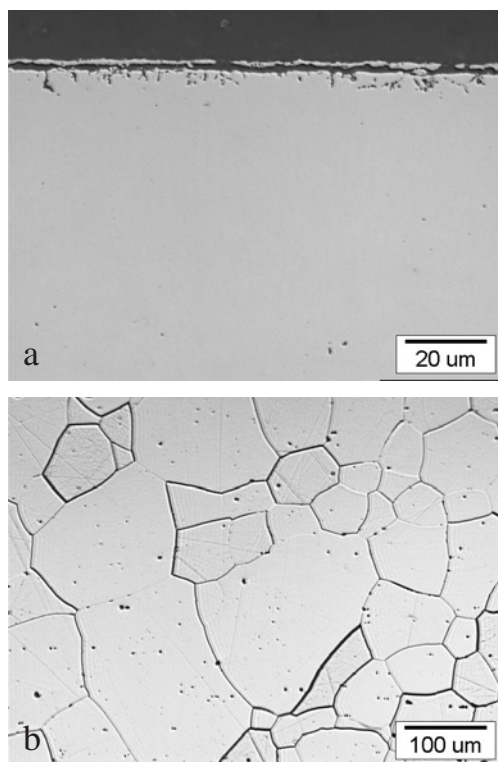
The oxidation of the Fe-Si-Al alloy with 0.01 % Cu during decarburization at $p(H_2O)/p(H_2) = 0.05$ started with the formation of a continuous oxide layer, which thickness increased parallely to the internal oxidation. The oxygen potential of the atmosphere is determined by the equation (1) and (2): [9]

$$H_2O = H_2 + \tfrac{1}{2}\,O_2 \tag{1}$$
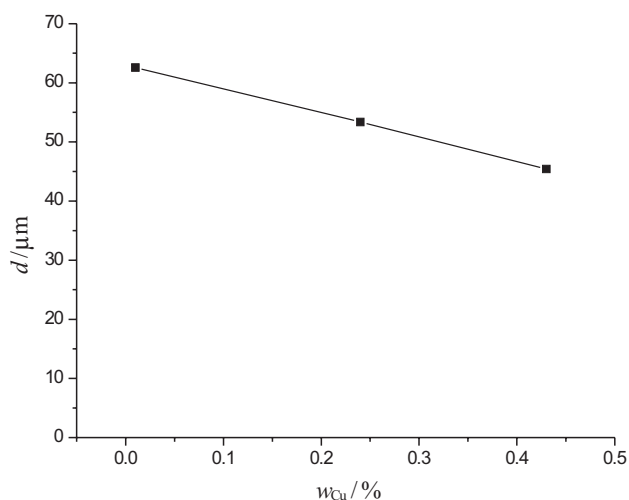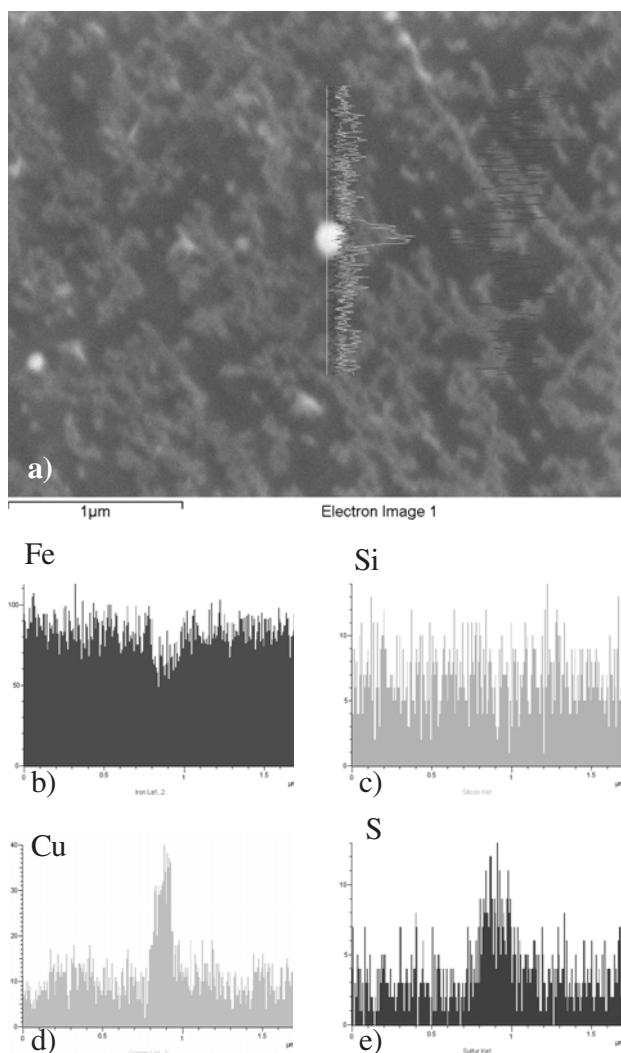
$$p(O_2) = k^2\,(p(H_2O)/p(H_2))^2 \tag{2}$$

At equilibrium conditions the $p(H_2O)/p(H_2)$ ratio corresponds the activity of oxygen on the reaction front gas mixture-metal.[9] It was confirmed [4,5,6] that inclusions formed in the metal during the decarburization of the Fe-Si-Al alloys consisted of Al and Si oxides.

On the other hand, the oxide layer on samples with higher copper contents (0.24 % and 0.43 %) appeared to offer protection against further diffusion of the oxygen at the grain boundaries, since no intergranular oxidation was observed. Since the solubility and the diffusivity of carbon in the oxides and oxide scales are extremely

Figure 4: Grain size as a function of the copper content in Fe-Si-Al alloys
Slika 4: Velikost zrn v zlitinah Fe-Si-Al v odvisnosti od vsebnosti bakra

Figure 5: Copper precipitate in the Fe-Si-Al alloy containing 0.43 % Cu; a) EDS – line scan of the precipitate, b) distribution of iron, c) distribution of copper, d) distribution of silicon, e) distribution of sulphur

Slika 5: Izloček bakra v zlitini Fe-Si-Al z 0,43 % Cu; a) EDS – linijska analiza izločka, b) porazdelitev železa, c) porazdelitev bakra, d) porazdelitev silicija, e) porazdelitev žvepla

small [10], it could be concluded that the oxidation of carbon was hindered by the oxide-scale formation.

The microstructure of the Fe-Si-Al alloys after heat treatment consisted of polyhedral ferrite grains (**Figures 1b, 2b, 3b**). In the alloy with 0.01 % Cu the grains were coarser (**Figure 3b**). The dependence of grain size versus copper content in the alloy is given in **Figure 4**.

The decrease of the grain size with the increase of the copper amount may be related to copper grain-boundary segregation. It is known that impurities slow down the grain growth in metals and alloys because of the

dragging effect of atoms on the migration of grain boundaries [11]. It was not possible to verify this assumption, because only transgranular fracture was obtained in all alloys. It is, however, possible that the grain boundary segregation of copper does not lower the grain to grain cohesion to a level lower than that for transgranular cleavage.

The impurities can also effect the grain boundary migration when are in the form of dispersed phase. The precipitates retard the boundary migration [11] proportionally to their number per volume unity of the alloy. In accordance with the Fe-Cu phase diagram [12] the copper precipitates were observed (0.15 µm) in the microstructure of the alloys with higher copper content (**Figure 5**). An increased content of sulphur was determined with EDS analysis. It is therefore possible that the inclusions do not consist only of pure copper, but of copper sulphide.

4 CONCLUSIONS

- The decrease of the initial content of carbon was the highest in the Fe-Si-Al alloy with the lowest amount of copper.
- The residual carbon content in the Fe-Si-Al alloys after decarburization is independent on the copper content in the range of mass fraction of Cu from 0.01 % to 0.43 %.
- The recrystallized grain size in the Fe-Si-Al alloy decreased by increasing the content of copper in the alloy. The smaller grain size in these alloys could be associated with the presence of copper precipitates and to the copper boundary segregation.

5 REFERENCES

[1] H. J. Grabke, G. Tauber, Arch. Eisenhüttenwes., 46 (**1975**) 3, 215–222

[2] U. Wiesner, Neue Hütte, 31 (**1986**) 9, 330–333

[3] G. Lyudkovsky, A. G. Preban, J. M. Shapiro, J.Appl. Phys., 53 (**1982**) 3, 2419–2421

[4] D. Steiner Petrovič, M. Jenko, F. Vodopivec, H. J. Grabke, Kovine, zlit., tehnol., 31 (**1997**) 3–4, 209–211

[5] D. Steiner Petrovič, M. Jenko, V. Gontarev, H. J. Grabke, Kovine, zlit., tehnol., 32 (**1998**) 6, 493–496

[6] D. Steiner Petrovič, M. Jenko, H. J. Grabke, V. Prešern, Mater. tehnol., 35 (**2001**) 6, 337–341

[7] H. J. Grabke, G. H. Meier, Oxidation of Metals, 44 (**1995**), 147–176

[8] N. Morito, T. Ichida, Scripta Metallurgica, 10 (**1976**), 619–622

[9] P. Kofstad, A. Rahmel, R. A. Rapp, D. L. Douglass, Oxidation of Metals, 32 (**1989**), 125–166

[10] H. J. Grabke, Arch. Eisenhüttenwes., 44 (**1973**) 8, 603–608

[11] R. W. Cahn, P. Haasen, Physical Metallurgy, 4th Edition, North-Holland, Amsterdam, 1996

[12] T. B. Massalski, Binary Alloy Phase Diagrams, ASM, Materials Park, Ohio, 1990